

Maximal ratio combining performance analysis in practical Rayleigh fading channels

D.B. Smith and T.D. Abhayapala

Abstract: The authors present a novel theoretical method to analyse the maximal ratio combining (MRC) receivers using BPSK and M-PSK modulation in spatially correlated Rayleigh fading channels, with perfect and imperfect channel knowledge, in terms of antenna array configuration and parameters of scatterer distributions. In this analysis closed form expressions for error probabilities of these modulations with MRC are derived, allowing for non-distinct eigenvalues from the channel gain correlation matrix. The results of performance analysis assuming different receiver configurations and scattering scenarios presented give valuable insight into the performance of MRC in practical Rayleigh fading scenarios for isotropic and non-isotropic scatterer distributions.

1 Introduction

Maximal ratio combining represents a theoretically optimal combiner over fading channels as a diversity scheme in a communication system. Theoretically, multiple copies of the same information signal are combined so as to maximise the instantaneous SNR at the output [1]. However, system designs often assume that the fading is independent across multiple diversity channels. Physical constraints often restrain the use of antenna spacing required for independent fading across multiple antennas [2]. Therefore it is necessary to consider spatial correlation characteristics between the antennas.

Maximal ratio combining (MRC) of correlated fading signals with binary phase-shift keying (BPSK) has first been considered by Pierce and Stein in [3]. MRC of correlated fading signals with PSK modulation has been further considered in [4–7]. In [7] results are given for maximal ratio combining for complex Gaussian fading channels with correlated diversity for BPSK in Rician and Rayleigh fading. This paper extends the above work by establishing closed form expressions for performance in terms of the antenna array and scattering environment.

If we do not assume perfect channel knowledge, i.e. the channel coefficients are not known at the receiver, then they must be estimated either by the use of known pilot signals or in a blind manner. This can have a deleterious effect on the performance of MRC. Following from [8, 9] the physical characteristics of scatterer distributions and the antenna array inputs to the combiner are related to the performance of MRC in such typical scenarios assuming BPSK signalling.

In [10] expressions are given for the spatial correlation of distributions of scatterers which can be applied to various non-isotropic scatterer distributions over multiple antennas. In this paper the spatial correlation formulation in [10] is applied with maximal ratio combining of PSK modulation to typical antenna configurations for three to six receive antennas in two typical non-isotropic Rayleigh fading environments, and a Rayleigh isotropic scattering scenario. However, the method developed in this paper can be applied to an arbitrary number of antennas in an arbitrary geometry and for an arbitrary scatterer environment.

We develop a closed form expression for the bit error probability (BEP) for BPSK modulation, related to a generalised correlation function expression for perfect channel knowledge. Unlike the previous formulation, [3, 7], the closed form expression for the BEP allows for non-distinct eigenvalues in the covariance matrix of the channel gains. This is expanded to a closed form expression for the probability of symbol error (SEP) for M-PSK modulation where there may be non-distinct eigenvalues in the covariance matrix of the fading gains.

In recent work a closed-form expression for the BEP was derived for BPSK signalling and imperfect channel knowledge with distinct eigenvalues in the covariance matrix [8]. However, for the case of non-distinct eigenvalues in the covariance matrix a non-closed-form expression is used in [9]. The non-closed-form expression also applies when the pilot signal-to-noise ratio (SNR) equals the data SNR.

2 System model

Let us consider the operation of an L -branch maximal ratio combiner (MRC) on correlated Rayleigh fading channels. The combiner input from the ℓ th branch of an L branch MRC receiver is given by

$$y_\ell(t) = g_\ell(t)u(t) + n_\ell(t) \quad (1)$$

where $g_\ell(t)$ is the complex Gaussian channel gain, $u(t)$ is the transmitted information signal and $n_\ell(t)$ is the additive white Gaussian noise (AWGN).

Let us write the vector of channel gain $\mathbf{g} = [g_1, \dots, g_L]^T$, the vector of noise $\mathbf{v} = [n_1, \dots, n_L]^T$, and the vector of the received signal $\mathbf{y} = [y_1, \dots, y_L]^T$. For a Rayleigh fading

channel $\mathbf{g} \sim N_C(\mathbf{0}, \boldsymbol{\Sigma})$ has a zero mean complex Gaussian distribution with covariance $\boldsymbol{\Sigma} = E\{\mathbf{g}\mathbf{g}^\dagger\}$ where $E\{\cdot\}$ denotes the mathematical expectation and \cdot^\dagger denotes the complex conjugate transpose. Also note that $\mathbf{v}_n \sim N_C(\mathbf{0}, \sigma_v^2 \mathbf{I}_L)$, where σ_v^2 is the equal noise variance at each branch and \mathbf{I}_L is the identity matrix of size L .

Let $\hat{\mathbf{g}}_\ell$ be the estimate of the channel gain of the ℓ th finger and $\hat{\mathbf{g}}_\ell = [\hat{g}_1, \dots, \hat{g}_L]$. In MRC, the signal received from each decision branch is multiplied by the complex conjugate of the corresponding estimate of channel gain and summed together to give a decision variable:

$$d(t) = \hat{\mathbf{g}}^H \mathbf{y} \quad (2)$$

Since only a quasi-static analysis is being applied in this paper we discard the time index from this point forward.

2.1 Spatial correlation

In this Section we show the connection between the elements of the covariance matrix $\boldsymbol{\Sigma}$ of the channel gains and the spatial correlation of the signal received at the two branches of the combiner.

Let the ℓ th and ℓ' th antennas be located at points \mathbf{x}_ℓ and $\mathbf{x}_{\ell'}$. Then the spatial correlation between the received signal (without noise) at the ℓ th and ℓ' th antennas is given by

$$\rho_{\ell,\ell'} = \frac{E\{z_\ell z_{\ell'}^*\}}{\sqrt{E\{|z_\ell|^2\}E\{|z_{\ell'}|^2\}}} \quad (3)$$

where $z_\ell = g_\ell u$. By assuming slow fading, it can be shown that

$$\rho_{\ell,\ell'} = \frac{E\{g_\ell g_{\ell'}^*\} \sigma_u^2}{\bar{\gamma} \sigma_v^2} \quad (4)$$

and similarly

$$\bar{\gamma} = \frac{\sqrt{E\{|g_\ell|^2\}E\{|g_{\ell'}|^2\}} \sigma_u^2}{\sigma_v^2} \quad (5)$$

where $\bar{\gamma} = \gamma_\ell$, and thus $E\{|g_\ell|^2\} = E\{|g_{\ell'}|^2\}$, for all ℓ , is the equal average SNR at the input to each branch, σ_u^2 is the transmitted signal power and σ_v^2 is the equal noise power at each branch. Without loss of generality we assume $\sigma_u^2 = 1$, and $\sigma_v^2 = 1$ for mathematical convenience.

Now we use (4) to express elements of the covariance matrix ($\boldsymbol{\Sigma} = E\{\mathbf{g}\mathbf{g}^\dagger\}$) of channel gains as

$$\boldsymbol{\Sigma}(\ell, \ell') = \bar{\gamma} \rho_{\ell,\ell'} \quad (6)$$

In physical channel modelling, if the scattering field is restricted to the horizontal plane, the correlation between the received signal at two branches is given, [10], by

$$\rho_{\ell,\ell'} = \sum_{m=-\infty}^{\infty} j^m C_m J_m(k \|x_\ell - x_{\ell'}\|) e^{jm\phi_{\ell,\ell'}} \quad (7)$$

where $J_m(\cdot)$ is the m th order Bessel function of the first kind, $k = 2\pi/\lambda$, $\phi_{\ell,\ell'}$ is the angle of the vector connecting x_ℓ and $x_{\ell'}$ and

$$C_m = \int_0^{2\pi} P(\phi) e^{-jm\phi} d\phi \quad (8)$$

where $P(\phi)$ is the normalised average power received from the direction ϕ . Common angular power distributions are the (i) Von Mises, (ii) Laplacian, (iii) Gaussian and (iv) uniform limited azimuth distribution and the corresponding sets of C_m are derived in [10]. For the Von Mises

distribution we have

$$C_m = e^{-jm\phi_0} \frac{I_{-m}(\kappa)}{I_0(\kappa)}$$

where $I_m(\kappa)$ represents the modified Bessel function of the first kind, κ is a parameter representing the degree of nonisotropy and ϕ_0 represents the mean direction. For the Laplacian distribution we have

$$C_m = e^{-jm\phi_0} \frac{(1 - (-1)^{\lceil m/2 \rceil} \xi F_m)}{(1 + \sigma^2 m^2 / 2)(1 - \xi)}$$

where $\xi = e^{-\pi/(\sqrt{2}\sigma)}$; $F_m = 1$ for m even; and $F_m = m\sigma/\sqrt{2}$ for m odd. Both the Laplacian and Von Mises distributions will be analysed in Section 5.

In the remainder of the paper we use (6) and (7) to derive performance analysis expressions in terms of antenna array configuration and parameters of scatterer distributions.

3 Bit-error-probability (BEP) of BPSK signalling with MRC

For BPSK, let the transmitted data information symbols in (1) be $u(t) \in \{+\sigma, -\sigma\}$.

3.1 BEP of BPSK with perfect channel knowledge

Let us consider the case where we have perfect channel-state information. Then the channel estimate $\hat{\mathbf{g}} = \mathbf{g}$.

The bit-error-probability (BEP) of the MRC can be given as [7]:

$$P_b = \frac{1}{\pi} \int_0^{\pi/2} \left[\det \left(\frac{\boldsymbol{\Sigma}}{\sin^2 \theta} + \mathbf{I} \right)^{-1} \right] d\theta \quad (9)$$

where $\boldsymbol{\Sigma} = E\{\mathbf{g}\mathbf{g}^\dagger\}$ as defined previously. In the L -branch combiner suppose $(1/\bar{\gamma})\boldsymbol{\Sigma}$ has N distinct eigenvalues, $\lambda_1, \dots, \lambda_N$ such that $N \leq L$; then following from [7], where now we are accounting for a possible multiplicity of eigenvalues,

$$\left[\det \left(\frac{\boldsymbol{\Sigma}}{\sin^2 \theta} + \mathbf{I} \right)^{-1} \right] = \sum_{n=1}^N \sum_{s=1}^{m_n} b_{s,n} \left(\frac{\bar{\gamma} \lambda_n}{\sin^2 \theta} + 1 \right)^{-s} \quad (10)$$

where m_n is the multiplicity of each eigenvalue λ_n , such that $\sum_{n=1}^N m_n = L$ and, using a result from [11], the n th residue of multiplicity s , $b_{s,n}$, is

$$b_{s,n} = \frac{\left\{ \frac{d^{m_n-s}}{dx^{m_n-s}} \prod_{i \neq n} \left(1 - \frac{\lambda_i}{x} \right)^{-m_i} \right\}_{|x=\lambda_n}}{(m_n - s)! c_n^{m_n-s}} \quad (11)$$

where $c_n = \bar{\gamma} \lambda_n$.

From (9) we then have

$$P_b = \frac{1}{\pi} \int_0^{\pi/2} \sum_{n=1}^N \sum_{s=1}^{m_n} b_{s,n} \left(\frac{c_n}{\sin^2 \theta} + 1 \right)^{-s} d\theta \quad (12)$$

We use a result from [12],

$$\frac{1}{\pi} \int_0^{\pi/2} \left(\frac{c_n}{\sin^2 \theta} + 1 \right)^{-s} d\theta = P_n(c)^s \sum_{k=0}^{s-1} \binom{s-1+k}{k} \times [1 - P_n(c)]^k \quad (13)$$

where

$$P_n(c) = \frac{1}{2} \left(1 - \sqrt{\frac{c_n}{1+c_n}} \right)$$

to obtain the following expression for P_b :

$$P_b = \sum_{n=1}^N \sum_{s=1}^{m_n} b_{s,n} P_n(c)^s \sum_{k=0}^{s-1} \binom{s-1+k}{k} [1 - P_n(c)]^k \quad (14)$$

When there is independent and identically distributed (i.i.d.) Rayleigh channel fading (14) reduces to [13, Eqn. (27)].

We can use (4) and (5) to theoretically construct correlation matrices for different scatterer distributions. After calculation of eigenvalues from the constructed correlation matrix we can use (14) to theoretically evaluate MRC performance against different scatterer distributions and geometries.

3.2 BEP of BPSK with MRC and imperfect channel knowledge

In this Section, we assume that the receiver does not have perfect channel state information. The noisy channel estimate $\hat{\mathbf{g}}$ is obtained by maximum-likelihood (ML) channel estimation using a block of M pilot symbols $u_t^{(p)} \in \{\sigma_p, -\sigma_p\}$ with variance σ_p^2 . This is given in [14]:

$$\hat{\mathbf{g}} = \mathbf{g} + \frac{1}{M\sigma_p^2} \sum_{t=0}^{M-1} u_t^{(p)*} n(t) \quad (15)$$

where as in the previous section $n(t)$ represents AWGN.

The following bit error probability for BPSK is given from the closed form expression derived in [8] assuming distinct eigenvalues in the correlation matrix. The subsequent derivation, which gives a non-closed-form expression, [9], is for the case where there may be non-distinct eigenvalues in the correlation matrix.

If we define

$$\mathbf{r}_n = \begin{bmatrix} \hat{\mathbf{g}}_n \\ \mathbf{y}_n \end{bmatrix}, \mathbf{A} = \frac{1}{2} \begin{bmatrix} 0 & 1 \\ 1 & 0 \end{bmatrix} \otimes \mathbf{I}_L \quad (16)$$

where \otimes is the Kronecker product, we obtain the $2L$ eigenvalues, μ_ℓ , of $\mathbf{A}\mathbf{K}_r$, where $\mathbf{K}_r = E\{\mathbf{r}_n \mathbf{r}_n^\dagger\}$ is the $(2L \times 2L)$ covariance matrix of \mathbf{r}_n . The decision variable can be expressed as $d_n = \mathbf{r}_n^\dagger \mathbf{A} \mathbf{r}_n$ in Hermitian quadratic form. Then, assuming distinct eigenvalues, the bit error probability is obtained from the pdf of d_n by integration as

$$P_b = \sum_{\substack{\ell=1 \\ \mu_\ell < 0}}^{2L} \prod_{\substack{k=1 \\ k \neq \ell}}^{2L} \frac{\mu_\ell}{\mu_\ell - \mu_k} \quad (17)$$

If there are non-distinct eigenvalues, μ_ℓ , or the eigenvalues are very closely spaced and hence the evaluation of (17) becomes numerically unstable, then the bit error probability (BEP) can be calculated directly from the characteristic function of d_n , [9], as

$$P_b = \frac{1}{2} - \frac{1}{\pi} \int_0^\infty \text{Im} \left\{ \frac{1}{\omega \prod_{l=0}^{2L-1} (1 - j\omega \mu_l)} \right\} d\omega \quad (18)$$

The eigenvalues, μ_ℓ , in (17) and (18) can be found from the eigenvalue decomposition of

$$\frac{1}{\bar{\gamma}} \begin{bmatrix} \boldsymbol{\Sigma} & \boldsymbol{\Sigma} + \mathbf{I}_L \\ \boldsymbol{\Sigma} + \frac{\bar{\gamma}}{\gamma_p} \mathbf{I}_L & \boldsymbol{\Sigma} \end{bmatrix} \quad (19)$$

where as in the previous section $\boldsymbol{\Sigma} = E\{\mathbf{g}\mathbf{g}^\dagger\}$, and

$$\gamma_p = \frac{\sigma_p^2}{\sigma_v^2} \quad (20)$$

represents the effective pilot-signal-to-noise ratio. Note that if $\gamma_p = \bar{\gamma}$ then (18) should be used rather than (17).

4 Symbol-error-probability of M-PSK with MRC and perfect channel knowledge

The results for the BEP of BPSK for MRC in a Rayleigh fading channel can be extended to the probability of symbol error (SEP) of M-PSK in a Rayleigh fading channel in a straightforward manner (this is for the assumption of spatial correlation with perfect channel knowledge). Following from [7], the probability, P_s , can be written for M-PSK in a Rayleigh fading channel as,

$$P_s = \frac{1}{\pi} \int_0^{(M-1)\pi/M} \left[\det \left(\frac{\boldsymbol{\Sigma} \sin^2(\pi/M)}{\sin^2 \theta} + \mathbf{I} \right) \right]^{-1} d\theta \quad (21)$$

If there is a possible multiplicity of eigenvalues, then P_s can be written as

$$P_s = \frac{1}{\pi} \int_0^{(M-1)\pi/M} \sum_{n=1}^N \sum_{s=1}^{m_n} b_{s,n} \left(\frac{\bar{\gamma} \lambda_n \sin^2(\pi/M)}{\sin^2 \theta} + 1 \right)^{-s} d\theta \quad (22)$$

Using a result from [12], we obtain the following result for P_s :

$$P_s = \frac{M-1}{M} - \sum_{n=1}^N \sum_{s=1}^{m_n} b_{s,n} \frac{1}{\pi} \sqrt{\frac{c_n}{1+c_n}} \left\{ \left(\frac{\pi}{2} + \tan^{-1} \alpha \right) \times \sum_{k=0}^{s-1} \binom{2k}{k} \frac{1}{[4(1+c_n)]^k} + \sin(\tan^{-1} \alpha) \times \sum_{k=1}^{s-1} \sum_{i=1}^k \frac{T_{i,k}}{(1+c_n)^k} [\cos(\tan^{-1} \alpha)]^{2(k-i)+1} \right\} \quad (23)$$

where $c_n = \bar{\gamma} \log_2 M \cdot \lambda_n \sin^2(\pi/M)$, considering that $\bar{\gamma}$ is the average SNR per bit on each channel and SEP is being evaluated; $b_{s,n}$ is as defined in (11),

$$a = \sqrt{\frac{c_n}{1+c_n}} \cot \frac{\pi}{M}$$

and

$$T_{i,k} = \frac{\binom{2k}{k}}{\binom{2(k-i)}{k-i}} 4^i [2(k-i)+1]$$

When there is i.i.d. Rayleigh channel fading, (23) reduces to [13, Eqn. (21)].

5 MRC with standard antenna configurations

In this section we analyse the performance of some standard antenna configurations as inputs to an $L=3$ to $L=6$ branch MRC in isotropic and some non-isotropic scattering scenarios based on the results of the previous Sections. Some general performance guidelines are obtained on the basis of the BEP for BPSK signals assuming both perfect and imperfect channel knowledge, and the SEP of 8-PSK modulation. Note that the theory applied in this paper can be applied to any number of antennas in any arbitrary geometry.

Here we consider the uniform circular array (UCA) and the uniform linear array (ULA). A range of antenna apertures in wavelengths, λ , are considered for the UCA, where the aperture is the diameter of the UCA. A range of antenna separations are considered for the ULA. For the non-isotropic distributions, various angular spreads, σ_a , defined as the square root of the variance of the particular distribution, are used in the analysis.

In all analyses we assume Rayleigh fading where the average bit SNR, or data SNR, on each of the L channels is considered to be the same, such that $\bar{\gamma}_\ell = \bar{\gamma}$, $\ell = 1, \dots, L$ (as stated previously). In addition $\bar{\gamma}$ is assumed to be 10 dB except where noted otherwise.

5.1 Analysis for BPSK signals with perfect channel knowledge

Figures 1–3 show the BEP of BPSK signals for an $L=3$ branch, $L=4$ branch and $L=6$ branch MRC with different

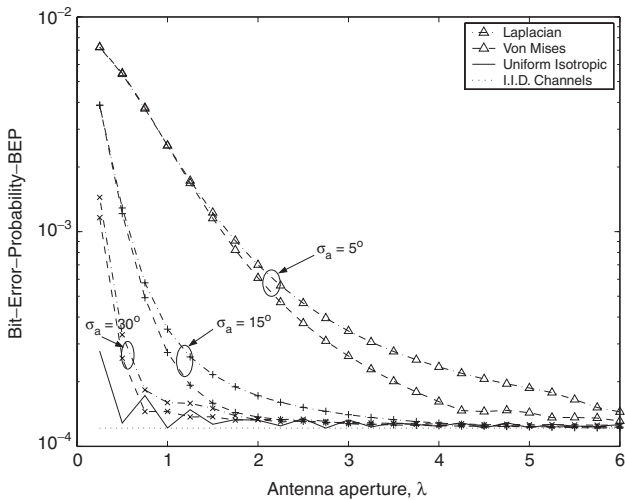


Fig. 1 Bit-error-probability (BEP) for an $L=3$ branch maximal ratio combining (MRC) of BPSK for Laplacian and Von Mises distributions of various angular spreads, σ_a , angle of incidence from broadside, $\beta=60^\circ$, and a uniform isotropic distribution

Inputs to the MRC are from a uniform circular array (UCA), with antenna aperture in wavelengths, λ . MRC for L i.i.d. channels is shown for reference. Average SNR per bit on the ℓ th channel, $\bar{\gamma}_\ell = 10$ dB

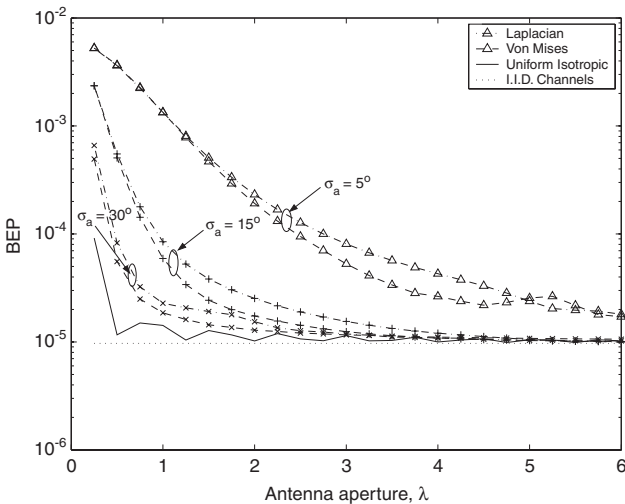


Fig. 2 BEP for $L=4$ branch MRC of BPSK for Laplacian and Von Mises distributions of various σ_a , $\beta=60^\circ$, and a uniform isotropic distribution, $\bar{\gamma}_\ell = 10$ dB

Inputs to the MRC are from a UCA. MRC for L i.i.d. channels is shown for reference

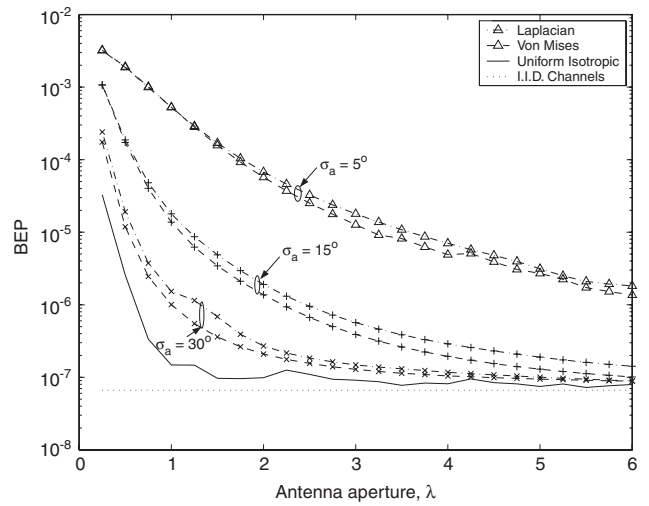


Fig. 3 BEP for $L=6$ branch MRC of BPSK for Laplacian and Von Mises distributions of various σ_a , $\beta=60^\circ$ and a uniform isotropic distribution, $\bar{\gamma}_\ell = 10$ dB

Inputs to the MRC are from a UCA. MRC for L i.i.d. channels is shown for reference

scattering scenarios using a UCA as input where there is perfect channel knowledge (thus the pilot SNR is effectively ∞ dB). In these three figures the angle of incidence from broadside is $\beta = 60^\circ$.

It is clear that for both non-isotropic scattering scenarios over a range of angular spreads there is a significant variation in the BEP. The BEP for an $L=4$ branch MRC shown in Fig. 2 is approximately 100 times greater for an angular spread $\sigma_a = 5^\circ$ compared with $\sigma_a = 30^\circ$ for both non-isotropic scatterer distributions at a UCA antenna aperture of 1λ . There is a similar trend of degradation from larger σ_a to smaller σ_a for Fig. 1 and Fig. 3.

It is demonstrated in Figs. 1–3 for the non-isotropic scattering scenarios, that even with a large angular spread there is degradation in the BEP when compared to that of a uniform isotropic distribution. The non-uniform improvement in the BEP of the uniform isotropic distribution as the antenna aperture increases, which is most pronounced in Fig. 2 for $L=4$, may be attributable to the shape of the zeroth order Bessel function of the first kind correlation model used for this distribution.

The results for the variation of BEP with angular spread in Figs. 1–3 for the non-isotropic scatterer distributions may be directly attributable to a decrease in the spatial correlation. In [15] a decrease in spatial correlation is shown as antenna spacing and/or angular spread increases for non-isotropic distributions. The small variation of the BEP for the same angular spread is also explained in [15] by the distribution variance dominating correlation, and not the choice of non-isotropic distribution.

The BEP for BPSK, with $L=6$ branch MRC using a ULA as input, which has a range of antenna separation (the distance in wavelengths, λ , between adjacent elements of the ULA) is shown in Fig. 4. Similar trends are displayed as compared with Figs. 1–3. However there are two noteworthy differences. Firstly, for smaller array sizes, Fig. 4 shows a larger variation in BEP between the non-isotropic scattering scenarios and the uniform scattering scenario. The second difference is a uniform improvement in the BEP where there is a uniform isotropic distribution for the ULA when compared with the UCA.

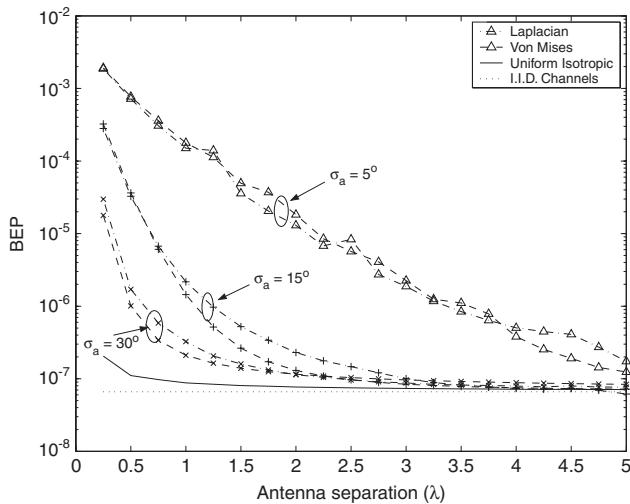


Fig. 4 BEP for $L=6$ branch MRC of BPSK for Laplacian and Von Mises distributions of various σ_a , $\beta=60^\circ$ and a uniform isotropic distribution, $\bar{\gamma}_\ell = 10$ dB. Inputs to the MRC are from a ULA. MRC for L i.i.d. channels is shown for reference

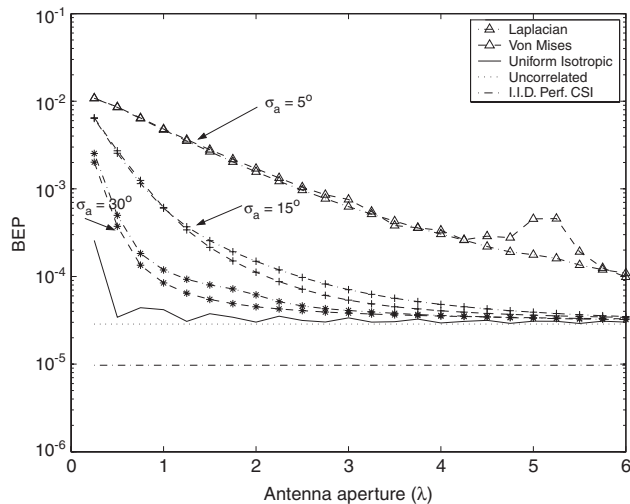


Fig. 6 BEP for $L=4$ branch MRC of BPSK for Laplacian and Von Mises distributions of various σ_a , $\beta=60^\circ$, and a uniform isotropic distribution, $\bar{\gamma}_\ell = 10$ dB, $\gamma_p = 15$ dB. Inputs to the MRC are from a UCA. MRC for L i.i.d. channels is shown for reference

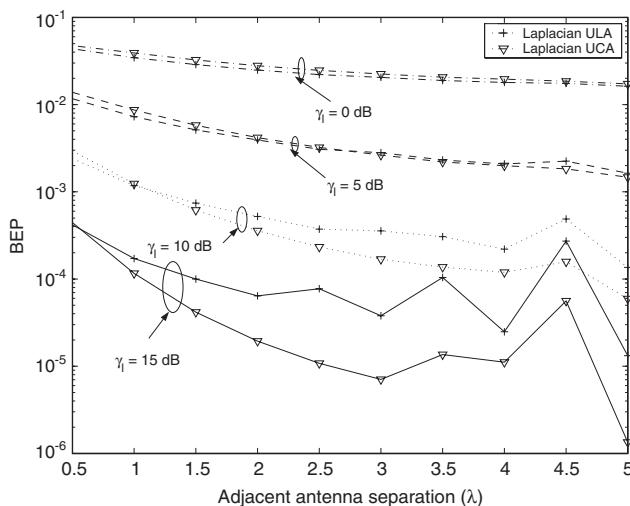


Fig. 5 BEP for $L=4$ branch MRC of BPSK for Laplacian distribution for $\sigma_a=5^\circ$, angles of incidence, β averaged over values from $[0, 2\pi)$, for varying data SNR, $\bar{\gamma}_\ell$. Inputs to the MRC are from a UCA and a ULA with uniform adjacent antenna separation, λ .

Figure 5 shows relative performance of a 4 element UCA and a 4 element ULA over angles of incidence to the MRC inputs averaged over $[0, 2\pi)$ for varying data SNR, $\bar{\gamma}_\ell$, for a Laplacian distribution at the UCA and ULA with an angular spread of 5° . At smaller data SNR there is virtually no performance variation between the UCA and ULA. However there is a more noteworthy relative improvement in performance of a UCA over a ULA as the adjacent antenna separation gets larger and the data SNR increases.

5.2 Analysis for BPSK signals with imperfect channel knowledge

Figure 6 shows similar trends to Fig. 2 for BEP of MRC without perfect channel knowledge with a pilot SNR, γ_p , of 15 dB and $L=4$ with all other parameters the same as in Fig. 2. There is a uniform reduction in bit-error-probability, with only a slight variation in the trend of degradation for $\sigma_a = 5^\circ$ at the larger antenna aperture.

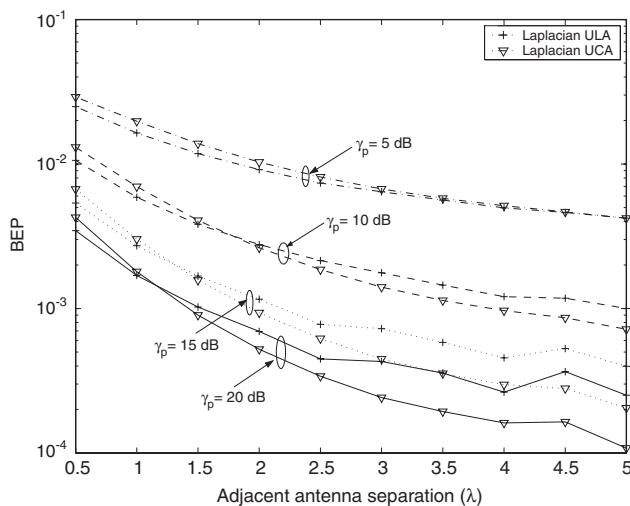


Fig. 7 BEP for $L=4$ branch MRC of BPSK for Laplacian distribution for $\sigma_a=5^\circ$, angles of incidence, β averaged over values from $[0, 2\pi)$, for varying pilot SNR, γ_p , with the average bit SNR (or data SNR), $\bar{\gamma}_\ell = 10$ dB, varying γ_p . Inputs to the MRC are from a UCA and a ULA with uniform adjacent antenna separation, λ .

Figure 7 shows the relative performance of a 4 element UCA and the ULA over angles of incidence to the MRC inputs averaged over $[0, 2\pi)$ for varying pilot SNR, γ_p , with the average bit SNR (or data SNR), $\bar{\gamma}_\ell$, fixed at 10 dB for a Laplacian distribution at the UCA and ULA with an angular spread of 5° .

Figure 7 illustrates that the performance of the UCA and ULA does not vary significantly over a range of adjacent antenna separation (λ) for the same γ_p (note that for a UCA the adjacent antenna separation is the minimum distance between array elements). However, performance improvement using a UCA becomes more significant than the improvement using a ULA as the pilot SNR increases and the adjacent antenna separation increases.

As in Fig. 5, Fig. 8 shows the relative performance of a 4 element UCA and a 4 element ULA over angles of incidence to the MRC inputs averaged over $[0, 2\pi)$ for varying data SNR, $\bar{\gamma}_\ell$. In Fig. 8, the pilot SNR, γ_p , is fixed

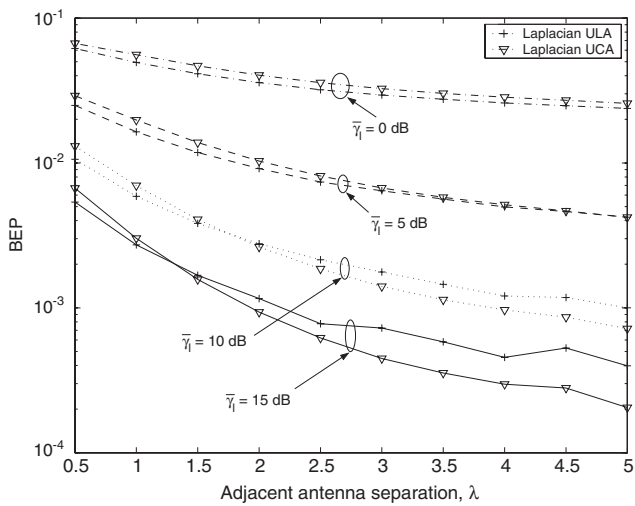


Fig. 8 BEP for $L=4$ branch MRC of BPSK for Laplacian distribution for $\sigma_a=5^\circ$, angles of incidence, β averaged over values from $[0, 2\pi)$, for varying data SNR, varying $\bar{\gamma}_\ell$, $\gamma_p = 10$ dB. Inputs to the MRC are from a UCA and a ULA with uniform adjacent antenna separation, λ

at 10 dB, for a Laplacian distribution at the UCA and ULA with an angular spread of 5° .

Importantly, this analysis shows a similar trend for Fig. 7 and Fig. 8 of performance improvement, of a UCA relative to the ULA, as the adjacent antenna separation increases. This trend is demonstrated for increasing pilot SNR in Fig. 7 and for increasing data SNR in Fig. 8. However in Fig. 8 the BER performance improvement is clearly less significant as the data SNR is increased. There is a more noticeable performance improvement in Fig. 5 for the case of perfect channel knowledge, $\gamma_p = \infty$ dB.

This analysis has been applied to a Laplacian distribution but this trend also appears to be applicable to other distributions, such as the Von Mises distribution, although this trend is only for a small angular spread, σ_a , at the array. At significantly larger angular spreads, $\sigma_a = 15^\circ$ for instance, shown in Fig. 9, with all other parameters the same as in Fig. 7, there is no noticeable improvement of a UCA over a ULA as pilot SNR increases or as antenna aperture increases.

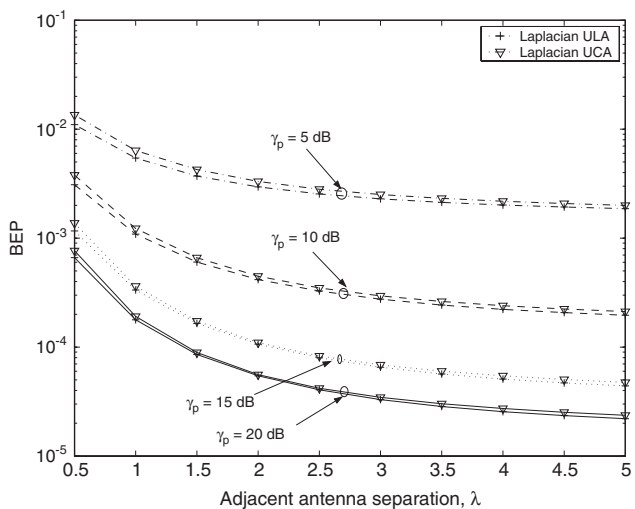


Fig. 9 BEP for $L=4$ branch MRC of BPSK for Laplacian distribution for $\sigma_a=15^\circ$, angles of incidence, β averaged over values from $[0, 2\pi)$, for varying data SNR, $\bar{\gamma}_\ell = 10$ dB, varying γ_p . Inputs to the MRC are from a UCA and a ULA with uniform adjacent antenna separation (λ)

5.3 Analysis for M-PSK signals with perfect channel knowledge

Figures 10 and 11 show very comparable trends for the symbol error probability (SEP) for 8-PSK modulated signals, to the BEP for BPSK signals with perfect channel knowledge, which is intuitive. Results using an $L=6$ branch UCA are shown in Fig. 10, and results for an $L=6$ branch ULA are shown in Fig. 11.

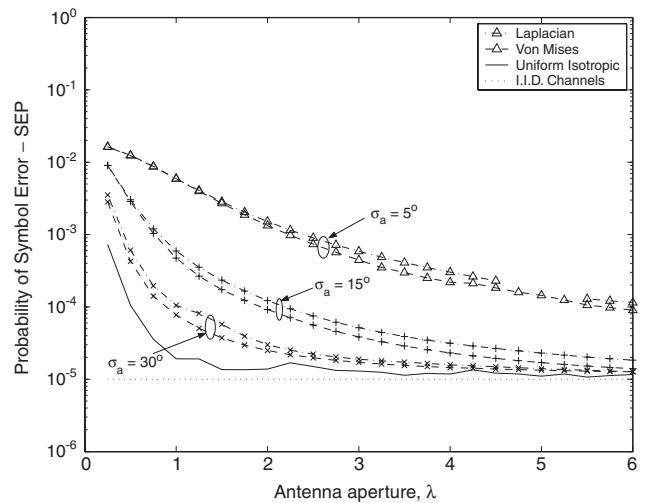


Fig. 10 SEP for $L=6$ branch MRC of 8-PSK for Laplacian and Von Mises distributions of various σ_a , $\beta=60^\circ$ and a uniform isotropic distribution, $\bar{\gamma}_\ell = 10$ dB

Inputs to the MRC are from a UCA. MRC for L i.i.d. channels is shown for reference

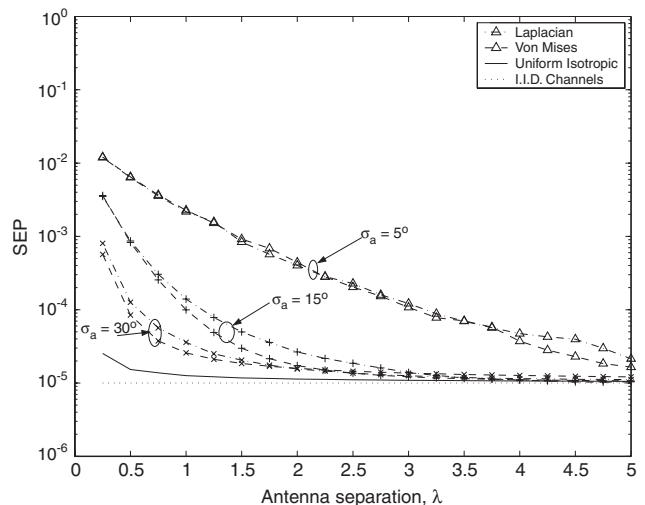


Fig. 11 SEP for $L=6$ branch MRC of 8-PSK for Laplacian and Von Mises distributions of various σ_a , $\beta=60^\circ$ and a uniform isotropic distribution, $\bar{\gamma}_\ell = 10$ dB

Inputs to the MRC are from a ULA. MRC for L i.i.d. channels is shown for reference

6 Conclusions

A theoretical method has been established to evaluate the performance of MRC receivers using BPSK and M-PSK modulation in correlated channels, in terms of antenna array geometry and scatterer distributions. Results of performance analysis for MRC, using PSK modulation in Rayleigh fading channels assuming spatial correlation at the receiver, have also been presented. This performance analysis accounts for the antenna configuration at the receiver, the size and shape of the configuration, and

the distribution of scatterers around the receiver. The results clearly demonstrate that there is a significant variation in performance when applying BPSK and M-PSK modulation over a range of angular spread for non-isotropic scattering scenarios. There is clear indication of the performance degradation due to spatial correlation at the receiver, dependent upon both the size and shape of the configuration, and whether there is isotropic or non-isotropic scattering in a Rayleigh fading channel.

Some variation in performance, although not large, between a ULA and a UCA is also indicated at small angular spreads for non-isotropic scattering scenarios. For a fixed number of antennas a ULA performs better for smaller array sizes, and a UCA for larger array sizes. This is indicated as the amount of channel knowledge increases for an increase in data SNR, and vice-versa. This trend is not repeated for larger angular spreads however.

The results outlined in this paper give useful insight into aspects of practical implementation of MRC in Rayleigh fading channels with typical antenna configurations and modulation schemes. It is hoped that more understanding of the effects of non-isotropy, antenna shape and size may lead to better implementations of receivers for MRC in Rayleigh fading channels.

7 Acknowledgments

National ICT Australia is funded through the Australian Government's Backing Australia's Ability initiative, in part through the Australian Research Council. This research is partially supported by the Australian Research Council grant DP0343804.

8 References

- 1 Brennan, D.: 'Linear diversity combining techniques', *Proc. IRE*, 1959, **47**, (1), pp. 1075–1102
- 2 Jakes, W.C.: 'Microwave mobile communications' (Wiley, New York, 1974)
- 3 Pierce, J.N., and Stein, S.: 'Multiple diversity with nonindependent fading', *Proc. IRE*, 1960, **4**, (1), pp. 89–104
- 4 Perahia, E., and Pottie, J.H.: 'On diversity combining for slowly flat-fading Rayleigh channels'. Proc. IEEE Int. Conf. on Communications, SUPERCOMM/ICC'94, New Orleans, USA, May 1994, Vol. 1, pp. 342–346
- 5 Abeysinghe, J.R., and Roberts, J. A.: 'Bit error rate performance of antenna diversity systems with channel correlation'. Proc. IEEE GLOBECOM'95, Singapore, November 1995, Vol. 3, pp. 2022–2026
- 6 Cho, Y., and Lee, J.H.: 'Effect of fading correlation on the SER performance of M-ary PSK with maximal ratio combining', *IEEE Commun. Lett.*, 1999, **3**, (7), pp. 199–201
- 7 Veeravalli, V.V.: 'On performance analysis for signaling on correlated fading channels', *IEEE Trans. Commun.*, 2001, **49**, (11), pp. 1879–1883
- 8 Dietrich, F.A., and Utschick, W.: 'Maximum ratio combining of correlated Rayleigh fading channels with imperfect channel knowledge', *IEEE Commun. Lett.*, 2003, **7**, (9), pp. 419–421
- 9 Schmitt, L., Grundler, T., Schreyoegg, C., Viering, I., and Meyer, H.: 'Maximum ratio combining of correlated diversity branches with imperfect channel state information and colored noise'. Proc. 2004 IEEE Int. Symp. on Spread Spectrum Techniques and Applications, ISSSTA 2004, Sydney, Australia, August 2004, pp. 859–863
- 10 Teal, P.D., Abhayapala, T.D., and Kennedy, R.A.: 'Spatial correlation for general distributions of scatterers', *IEEE Signal Process. Lett.*, 2002, **9**, (10), pp. 305–308
- 11 Simon, M.K., and Alouini, M.-S.: 'Digital communication over fading channels' (Wiley-IEEE, New York, 2004, 2nd edn.)
- 12 Alouini, M.S., and Goldsmith, A.: 'A unified approach for calculating error rates of linearly modulated signals over generalized fading channels', *IEEE Trans. Commun.*, 1999, **47**, (9), pp. 1324–1334
- 13 Chennakeshu, S., and Anderson, J.B.: 'Error rates for Rayleigh fading multichannel reception of MPSK signals', *IEEE Trans. Commun.*, 1995, **43**, (2), pp. 338–346
- 14 Poor, H.V.: 'An introduction to signal detection and estimation' (Springer-Verlag, 1994, 2nd edn.)
- 15 Pollock, T.S., Abhayapala, T.D., and Kennedy, R.A.: 'Introducing space into MIMO capacity calculations', *J. Telecommun. Syst.*, 2003, **24**, (2–4), pp. 415–436